Biophysical Chemistry 20 (1984) 185–200
Elsevier

BPC 00875

DYNAMIC LIGHT-SCATTERING STUDIES ON THERMAL MOTIONS OF NATIVE DNAs IN SOLUTION

Kunitsugu SODA and Akiyoshi WADA

Department of Physics, Faculty of Science, University of Tokyo, Hongo, Bunkyo-ku, Tokyo 113, Japan

Received 27th October 1983
Revised manuscript received 25th February 1984
Accepted 23rd March 1984

Key words: Light scattering; Dynamic light scattering; Thermal motion; Internal motion; Semiflexible chain; DNA

The basic character of dynamic light-scattering properties of native DNA was investigated on two DNA samples. The degree of non-single exponentiality of photocount correlation functions, $C(t)$, and its dependence on K are quantitatively characterized by two methods. The spectral linewidth, Γ_s, determined from $C(t)$ exhibits a K dependence near to but significantly different from the prediction for Rouse-Zimm (RZ) chains by Dubois-Violette and De Gennes: It is inferred from data on λ-DNA that the exponent in the K dependence of the spectral linewidth for native DNA takes a value larger than 3 in the K region corresponding to the 'K^3' region for RZ chains. These results are in good agreement with the prediction from the dynamic theory of semiflexible chains presented by one of us (K.S.). The apparent diffusion coefficients are fairly insensitive to DNA concentration and ionic strength at large K. On the other hand, it is indicated that the stiffness of native DNA may vary with temperature even in a temperature range substantially lower than that of melting.

1. Introduction

Application of the dynamic light scattering (DLS) method to study of the dynamic properties of polymer solutions was initially made to synthetic polymers. Most of the synthetic polymers have a persistence length much shorter than the reciprocal of the scattering vector, $1/K$, attainable by using a visible or ultraviolet laser, where

$$K = \frac{4\pi n}{\lambda} \sin\left(\frac{\theta}{2}\right), \tag{1}$$

and n, λ and θ are the refractive index of solution, the wavelength of light, and the scattering angle, respectively. Their DLS properties have been interpreted by applying the Rouse-Zimm (RZ) model. On the other hand, the double-stranded DNA molecule is a semiflexible polymer whose equilibrium properties are known to be well described by the worm-like chain model [1]. The value of $1/K$ can be comparable to the persistence length of native DNA in the DLS measurement at large scattering angles. Therefore, it is expected that the local motion of DNA segments with a length of the order of the persistence length is reflected in DLS properties. As a native DNA molecule has a finite torsional rigidity as well as a bending rigidity, its bending motion must be affected by its torsional motion. It is very interesting how the DLS properties of native DNA differ from those of flexible chains such as synthetic polymers.

DLS studies of double-stranded DNA first began by showing experimentally that not only translational motion but also intramolecular motion contributes to scattered-light spectra. Efforts to extract some parameters characterizing their motion from the form analysis of correlation functions have been made by several groups [2–4]. The dependence of the DLS properties of DNA on its conformational changes with binding of histones [5] and with temperature [6] were also measured.

Methods of data analysis used in these studies and results commonly obtained from them are summarized as follows. An apparent correlation time is obtained from fitting a single-exponential function to the correlation function measured at each angle. The reciprocal of the correlation time, being plotted vs. K^2, never lies on a straight line passing through the origin. This differs from the case of small particles such as globular proteins, where the correlation time is determined only from their translational motion. Because of this, measured correlation functions were analyzed assuming a single exponential function of the form

$$f(t) = A \exp\{-(2DK^2 + (1/\tau_i))t\}, \quad (2)$$

or a squared double exponential of the form

$$f(t) = [A_1 \exp\{-DK^2 t\} + A_2 \exp\{-(DK^2 + (1/\tau_i))t\}]^2. \quad (3)$$

The above τ_i terms were considered as quantities characterizing the internal motion of the DNA.

During the course of those works, several examples of abnormal behavior, such as the unexpectedly small value of the translational diffusion coefficient and the long tail of the correlation function, were reported [2–4,7]. In order to exclude the effect of the polydispersity of DNA samples, Jolly and Eisenberg [8] measured a well-fractionated sample of calf thymus DNA.

Chen et al. [9] also studied homogenized and unhomogenized samples extensively. They found no long relaxation times in the correlation functions for purified calf thymus DNA with a molecular weight up to 1.2×10^7, and established that the dominant lowest-frequency term originates from the translational motion of DNA. They analyzed data assuming several forms of correlation function including eq. 3. Applying Pecora's theory for RZ chains [10], they tried to deduce the value of the lowest-order relaxation time of the model from τ_i obtained from measurement. In spite of their precise measurements and careful analyses, neither Chen et al. nor Jolly could obtain any definite value of the relaxation time.

Lin and Schurr [11] also measured calf thymus DNA. They showed that the apparent diffusion coefficient obtained from a single exponential analysis reaches a stationary value in the region of K^2 greater than 5×10^{14} m^2/s. Assuming the above tendency of saturation, they proposed a method to extract a set of RZ model parameters. They applied it to their data for calf thymus DNA to give its RZ model parameters.

Voordouw et al. [12], who pointed out the importance of sample homogeneity, prepared ColEl DNA samples of supercoiled, open circular and linear forms. They measured the translational diffusion coefficient and the angular dependence of the apparent diffusion coefficient of each form of DNA.

Thomas et al. [13,14] prepared a carefully deproteinized ϕ29 DNA ($M_r = 1.15 \times 10^7$) samples and measured it using an ultraviolet laser to obtain correlation functions with no long tails. They applied the method of Lin and Schurr to the analysis of their data to estimate the values of RZ model parameters for the 'clean' DNA. Using the same method of analysis as the above, Lin et al. [15] investigated the effect of polycation binding to DNA and found that it facilitates local denaturation of DNA and induces titratable joints in DNA.

As reviewed above, there are as yet only a few data on homogeneous and purified samples. It is very difficult to compare quantitatively the data obtained by different experimenters. This is partially because, for want of an established method of data analysis, the respective investigators have used different methods. Almost no characterization has been made of the form of correlation functions themselves, and few discussions have taken place on the applicability of the RZ model. Taking account of this situation, we have measured purified DNAs to clarify the basic character of the DLS properties of native DNA molecules.

Recently, one of the authors presented a dynamic theory of circular semiflexible chains in which Berg's theory [16] was extended by including the effect of intramolecular hydrodynamic interaction and applied it to DLS problems [42]. Comparison of the experiment with this theory, hereafter referred to as the KS theory, will be made.

2. Materials and methods

2.1. DNA preparation and purification

We prepared two DNA samples, λ-DNA and ColEl DNA.

λ-phage was prepared from *Escherichia coli* M65 (λcI857s7) strain by the method devised by Goldberg and Howe [17] and modified by Dr. O. Gotoh (personal communication). After three cycles of low-speed ($6000 \times g$, 15 min) and high-speed ($60\,000 \times g$, 120 min) centrifugation, the phage was purified by banding it in a concentrated CsCl solution with three layers of increasing density. λ-DNA was extracted by the phenol extraction method repeated five times. Distilled reagent-grade phenol divided into flasks and stored shielded from light at 4°C was used for the extraction. The collected aqueous phase was exhaustively dialyzed against 1 × SSC buffer (0.15 M NaCl, 0.015 M trisodium citrate), and served as the stock solution for DLS measurements.

ColEl DNA was prepared from *E. coli* A745 met thy (ColEl) strain by a slightly modified method of Sakakibara and Tomizawa [18]. The plasmid DNA contained in a cleared lysate was deproteinized by phenol extraction three times. The extracted sample contained DNAs of not only a closed circular form, the major component, but also an open circular and a linear form as detected by gel electrophoresis. Only the closed circular component was collected by ethidium bromide (EtBr)-CsCl density gradient centrifugation. Linearized by restriction endonuclease *Eco*R1 and deproteinized by phenol, the sample was divided into two. Respective samples were extensively dialyzed against 5 × SSC and 1 × SSC buffer solutions and were used as stock solutions for DLS measurements.

The homogeneity of both DNA samples was examined by agarose gel electrophoresis. The buffer used in this step contained 40 mM Tris, 20 mM sodium acetate, 10 mM Na_2 EDTA, 5 μg/ml EtBr (pH 7.7). Each of the purified samples of λ-DNA and linearized ColEl DNA gave a clear single band. The ColEl closed circular DNA sample collected by density gradient centrifugation was found to contain an undetectable amount of linear DNA and less than 8% of the open circular form from a densitometer tracing of the gel. The fraction of open circular DNA is thus much smaller than that of closed circular DNA, and it can safely be assumed that most of the nicked DNAs among the linearized DNAs have only one nick in their contour length of about 2.24 μm, and that the effect of the nicks on the motion of DNA molecules is negligible.

The protein content was estimated to be less than 0.7% (w/w) of DNA by the method of Lowry et al. [19]. Each DNA sample showed a CD spectrum characteristic of B-form DNA. It was confirmed that each sample gave the same differential thermal melting profile as published data [20]. Both samples were used for experiments 2 weeks to 2 months after preparation.

As is well known, λ-DNA has cohesive ends and can take an open circular form [21]. To determine the form of our λ-DNA, a boundary-sedimentation velocity measurement was made for the DNA in 1 × SSC buffer at concentrations of 5 and 10 μg/ml. A clear single boundary was observed and the sedimentation coefficient, $s_{20,w}$, was found to be 39.2 S. Dawson and Harpst [22] reported the $s_{20,w}$ values of linear and circular λ-DNA as 34.2 and 40.5 S, respectively. The $s_{20,w}$ value of our sample is close to that of the circular λ-DNA of Dawson and Harpst. Therefore, it can be concluded that most of our λ-DNA takes the circular form under the conditions of 1 × SSC buffer and 25°C.

Samples for the DLS measurement were prepared by diluting stock solutions with appropriate buffers and making them dust-free as described in section 2.2. Concentrations of DNA were determined from measurements of absorbance at 260 nm and calculated using a value of $E^{0.1\%}_{1\text{ cm},260\text{ nm}} = 20.4$ according to Voordouw et al. [12].

2.2. Preparation of dust-free DNA solutions

The preparation of a dust-free sample solution is a crucial process that determines the accuracy and reproducibility of measured data in light-scattering measurements. As centrifugation is difficult to apply to high-molecular-weight DNA solutions, samples were cleaned exclusively by the

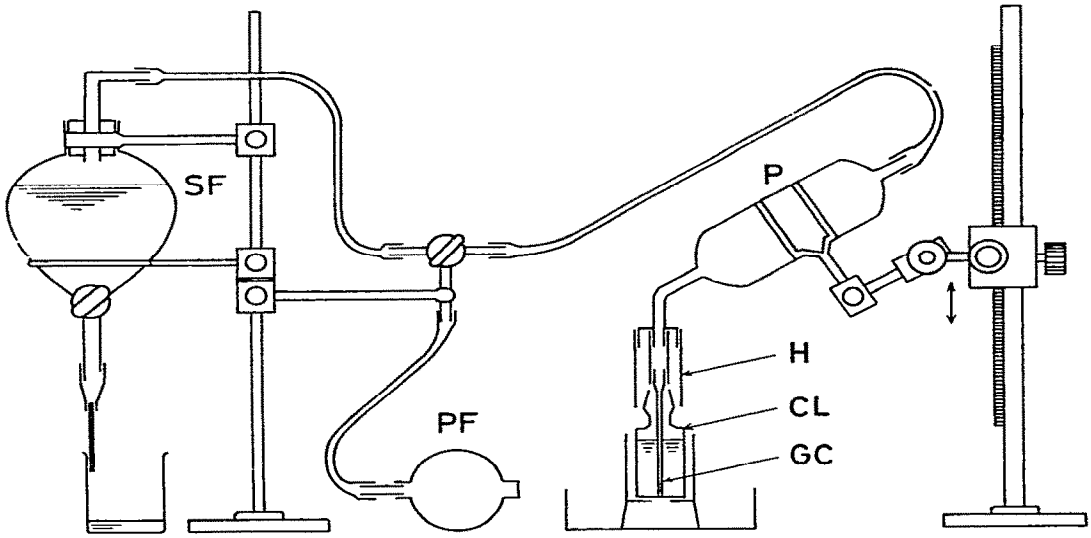

Fig. 1. Apparatus for drawing water or solvent from a sample cell to be cleaned. (P) Hand-made pipette, (H) silicon-rubber hood, (GC) glass capillary, (CL) sample cell, (SF) separating funnel, (PF) pipette filler. The pipette filler is used both for drawing the liquid from the cell in place of the separating funnel and for pushing out the liquid drawn up in the pipette.

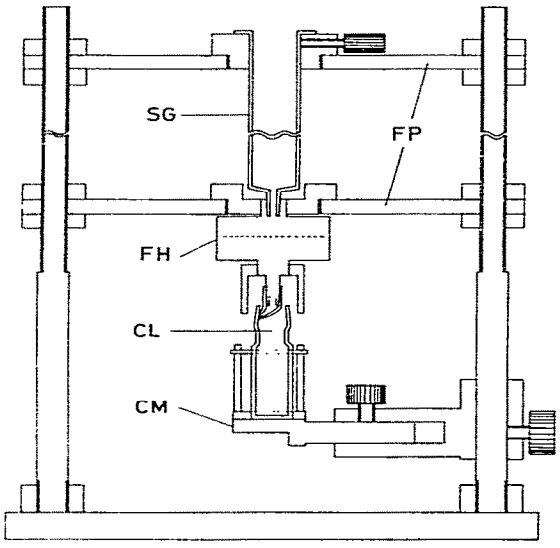

Fig. 2. Sample-filtration equipment (SFE). (FP) Fixed plates, (SG) plastic syringe, (FH) filter holder, (CL) sample cell, (CM) cell mount which can adjust the position of the sample cell so that the end of the polyethylene tube connected to the filter holder can contact the inner surface of the mouth of the cell.

filtration method [23]. The special devices in figs. 1 and 2 were made, and a relatively good reproducibility of cleaned samples could be obtained with this use.

The process of making a dust-free sample is as follows. Sample cells are generally stored in a 1% solution of neutral detergent. Only quartz cells are used, since pyrex cell walls often become muddy when they are kept for several months even in a neutral detergent solution. Taken out of the solution, the cell is extensively rinsed with hot water and then soaked in a chromic acid mixture for about 3 min. The cell is then rinsed with triply distilled dust-free water several times. After filling with dust-free water, the water is drawn up into a hand-made pipette (P) with a volume of 30 ml using the apparatus in fig. 1. This draws the water without disturbing the surface of water by maintaining a gentle inflow of air. The end of the pipette is connected to a glass capillary (GC) by a rubber tube. After inserting the capillary slowly into the cell, the water is drawn up by dripping water from a separating funnel (SF). The silicon-rubber hood (H) is appended to prevent dust

particles falling into the cell. The above processes are repeated about ten times. In our experience, obtaining a clean cell by carefully following the above procedures is an important step in making a dust-free sample.

The sample filtration equipment (SFE) in fig. 2 is composed of two fixed plates (FP) and a cell mount (CM). A plastic syringe (SG) can be fixed to the upper fixed plate. The filter holder (FH) is generally dismantled and stored in an alkaline detergent solution. After rinsing with hot water and dust free water, it is reassembled and furnished with a membrane filter. Nucleopore polycarbonate membrane filters are used because of the uniform pore size and short filtration time due to their thinness. About 60 ml dust-free water and 20 ml solvent are filtered to rinse the membrane filter and the holder. It was found more effective to rotate the syringe held at a slight angle during filtration. After the syringe and holder are installed on the sample filtration equipment, the solvent is filtered into the cleaned cell. The solvent is drawn as described above, and then the sample solution is filtered into the cell to give a dust-free sample for the DLS measurement.

Using the sample filtration equipment, filtering of a sample can be performed without causing any disturbance to the filtrate. The filtration of a DNA sample takes about 5 min to give 2.5 ml of filtrate under a pressure difference of less than 15 g/cm^2. It is important that the filtrate not be dropped into the cell and that air not be introduced into the inlet side of the filter holder for smooth filtering under a small pressure difference.

The pore sizes of the membrane filters used are 0.4 μm for λ-DNA, and 0.2 and 0.4 μm for ColEl DNA. It was confirmed that there was no change in the agarose gel electrophoresis pattern of either sample before and after filtering.

The quality of a cleaned sample was examined by observing the forward scattering of the white light from a projector lamp focused into the cell. When the sample is made completely dust-free, the light path in the cell is seen as a uniform pale band. If the sample contains some dust particles, they are easily detected because they produce strong Tyndall scattering.

2.3. Refractive index and viscosity of solvents

The refractive index of solvents at 589 nm was measured with an Abbe refractometer. The temperature of the samples was regulated to be the same as that in light-scattering measurements with an accuracy of 0.05 °C. The refractive index at the wavelength of an He-Ne laser (632.82 nm) was calculated assuming that it has the same dependence on wavelength as the refractive index of water [24].

Viscosity measurements on water and solvents were made with a Zimm-Crothers rotating viscometer and an Ubbelohde Capillary viscometer at several temperatures regulated to an accuracy of 0.02 °C. The solvent viscosity was calculated from the measured ratio of the viscosities of the solvent and water, and the published value of the viscosity of water at each temperature. From the reproducibility of measurement in each viscometer and the agreement between measured values from the two viscometers, the relative error of viscosity values is estimated to be less than 0.2%.

There are many papers in which the accuracy of solvent viscosity or measuring temperature is not explicitly indicated. The viscosity of water has a temperature coefficient of about 1%/0.1°C near 25 °C. Because the change of a correlation function relative to a change in external conditions is generally small, as described later, the accuracy of viscosity in the temperature viscosity factor, η/T, is important in reducing a measured value of the apparent diffusion coefficient to a value under the standard conditions of 25 °C in water.

2.4. DLS measuring system

The DLS measuring system composed of an optical system and a digital correlator is of our own making.

The light source is a 50 mW He-Ne laser (Nippon Electric Co. model GLG108). The rotatory arm, on which optical parts for scattered-light detection are mounted, is driven by a stepping motor, and the scattering angle can be set to between 0 and 150° in units of 0.01°. The accuracy of the scattering angle, which is limited by the accuracy of determination of the 0° position, is

estimated to be better than 0.08°.

The specially made sample cell (10(width)× 25(height)× 15(depth) mm) has a unique feature in that the walls through which the incident light passes make an angle of 1° with each other. This configuration is particularly effective in the measurements of backward scattering. It serves to exclude the contamination of strongly scattered light due to the incident light reflected on the cell wall on the exit side into weak backward-scattered light. The above configuration of our cell necessitates, in principle, a correction to the scattering angle. However, it can be neglected in the range of measuring angles larger than 8° taken in our study.

The sample cell is placed in a brass cell holder which has a nearly semicircular opening to permit the scattered light to pass through, and whose temperature is regulated by circulating water from a temperature-controlled bath. The accuracy of the cell temperature determined by the accuracy of temperature control of the water bath is 0.05°C near room temperature and 0.03°C at other temperatures in the range 10–60°C.

The computer-assisted digital correlator with 128 delay channels has a unique dust-effect reduction capability. This facility is very effective in the measurement of high-molecular-weight DNA in the following circumstances. (1) At a large scattering angle where the intensity of scattered light is very weak, usually more than 1 h is taken for the measurement of a correlation function. Without this facility, a single transit of a giant dust particle through the scattering volume could have a serious effect on measured data. The weaker the intensity, the longer will be the measuring time required, increasing the probability of the transit of dust particles. (2) As the correlation function is generally of a non-single-exponential form as described later, it is impossible to eliminate the effect of dust in the step of data analysis.

Details of the construction of the correlator and the use of our DLS system will be described elsewhere.

2.5. Data analysis

We have no theoretical expression for the dynamic structure factor of worm-like chains in which the effect of intramolecular hydrodynamic interaction is taken into account. Maeda and Fujime [25] presented a theory of DLS for semiflexible chains with no regard to the hydrodynamic interaction effect. Inclusion of the above effect into the theory of DLS is essential to make quantitative comparison of the theory with DLS data. On the other hand, the applicability of the RZ model taken exclusively so far for DNA is in doubt as explained below. Therefore, as it is the simplest way, we fitted a single exponential function of the form

$$f_{se}(t) = A \exp(-2D_a^* K^2 t) + B \tag{4}$$

to the measured correlation function, $C(t)$, as done by Lin and Schurr [11]. The computer fitting was made using a nonlinear least-squares routine based on the algorithm developed by Fletcher and Powell [26]. D_a^* in eq. 4 represents the apparent diffusion coefficient.

As described in section 3, $C(t)$ has an approximately single exponential form, but deviates significantly from it at those angles where intramolecular motion cannot be neglected. Accordingly, the fitted value of D_a^* generally depends on the range of delay time taken in the fitting. Though the range has been taken arbitrarily by various investigators, it should be specified to characterize data quantitatively. We performed the following procedure. The minimum delay time, t_d, is selected so that the value of the correlation function at the maximum delay time of the 128-th channel is slightly less than $1/100$ of that at zero delay time, hereafter referred to as the correlation amplitude. In the computer analysis, a fourth-order cumulant fitting,

$$f_{C4}(t) = A_4 \exp\{-K_1 t + (K_2/2)t^2 - (K_3/6)t^3 + (K_4/24)t^4\}, \tag{5}$$

is first made to the whole correlated data. The above fitting function was chosen because, for most of our data, a cumulant fitting of higher than the fourth order hardly improved the quality of fitting. The delay time, t_e, at which $C(t)$ is $1/100$ of the correlation amplitude, is estimated from the fitted function. Then only those data with delay times shorter than t_e are used for fitting the function of eq. 4. The case in which B is varied and

that in which it is fixed to zero are examined. By defining δ by A and B obtained from the former analysis as

$$\delta = B/(A+B), \tag{6}$$

it can be used as the quantity that characterizes the non-single exponentiality of $C(t)$.

The cumulant method commonly used to obtain the mean diffusion coefficient [27] was not adopted here in the following circumstances. Our photomultiplier gives a correlation function of dark current and white light with a correlation time of about 3 μs. This is considered to be due to the after-pulse effect. Because of this effect, the correlation function is superposed by a spurious component in the delay time region shorter than about 15 μs. As it is difficult to evaluate the magnitude of the component accurately, its contribution cannot in practice be subtracted from the measured value of $C(t)$. For both DNA samples, the number of pertinent channels is only three even at the largest angle. However, it was found that, when the data of a few initial channels were discarded, the value of the apparent diffusion coefficient could decrease by a non-negligible amount because of the non-single-exponential nature of the correlation function. Therefore, the following approximation was made. The function

$$f_{C2}(t) = A_2 \exp\{-K_1 t + (K_2/2)t^2\} \tag{7}$$

is first fitted to the data of the 10 channels subsequent to the pertinent ones. This is equivalent to a second-order cumulant fitting. Then, the values of the correlation function at the relevant channels and the correlation amplitude are estimated by extrapolating the fitted function.

The apparent diffusion coefficient, D_a, reduced to the value in the standard state of water at 25 °C is obtained from D_a^* as

$$D_a = \frac{298.15\eta}{8.949T} D_a^*, \tag{8}$$

where T (in K) is the measuring temperature and η (in mP) is the viscosity of solvent at that temperature.

For later discussion, we will briefly summarize the results of the KS theory. Theoretically, the DLS properties of a dilute polymer solution can be derived from the dynamic structure factor, $S(\boldsymbol{K},t)$, of the polymer. The theory gives $S(\boldsymbol{K},t)$ as

$$S(\boldsymbol{K},t) = 2L\alpha^2 \exp(-D_0 K^2 t) \int_0^{L/2} \mathrm{d}s\, c(\boldsymbol{K},s,t), \tag{9}$$

where

$$c(\boldsymbol{K},s,t) = \exp\left[-\sum_{n=1}^{\infty} \frac{4kTK^2}{3L\lambda_n} \times \left\{ 1 - \cos\left(\frac{2\pi s}{L} n \right) e^{-t/\tau_n} \right\} \right], \tag{10}$$

L, α and D_0 being the contour length of the semiflexible polymer, the polarizability per unit length, and the translational diffusion coefficient, respectively. λ_n, which is a function of the elastic constants of the chain and the temperature, is a quantity equivalent to the 'spring' constant for the n-th normal mode. τ_n is the relaxation time of the n-th mode and given by

$$\tau_n = \zeta_n/\lambda_n, \tag{11}$$

where ζ_n is the friction coefficient of the n-th mode. The intramolecular hydrodynamic interaction determines the dependence of ζ_n on mode number, n. As the measured $C(t)$ is related to $S(\boldsymbol{K},t)$ as

$$C(t) \propto |S(\boldsymbol{K},t)|^2, \tag{12}$$

the quantities such as D_a and D_s, which are introduced in the following section, can be evaluated using the above formula of $S(\boldsymbol{K},t)$. In the numerical calculations, the chain diameter was assumed to be 2.5 nm which was estimated by Yamakawa and Fujii [28] as the best value.

It must be noted here that, although the KS theory takes into account the effects of the bending stiffness and the hydrodynamic interaction for semiflexible chains fairly well, it still contains several assumptions and approximations as follows: (1) The longitudinal stiffness in the direction of the chain axis is introduced in an incomplete way; (2) the effect of torsional stiffness is not included; and (3) the excluded volume effect is not taken into account.

3. Results and discussion

3.1. Shape of correlation functions

In order to illustrate the K dependence of the shape of $C(t)$, typical correlation functions of ColEI DNA at three scattering angles are plotted semilogarithmically in fig. 3. The plot of $C(t)$ at the smallest angle of $\theta = 11.48°$ is almost linear, indicating that the contribution of the translational motion of DNA molecules dominates $C(t)$ at this angle. The plot has no long tail as was frequently observed earlier in correlation functions at small angles for calf thymus DNA. This result also shows that our DNA samples are well purified. As the scattering angle increases, intramolecular motion other than translational begins to contribute to $C(t)$. From the plot of $\theta = 36.87°$, the effect of intramolecular motion is seen to appear first as a deviation of $C(t)$ from a single exponential form at short delay times. At $\theta = 90.00°$, the semilogarithmic plot of $C(t)$ is not linear over the entire delay time region.

In order to represent quantitatively the above dependence of the non-single-exponential character of the correlation function on scattering angle, δ given by eq. 6 is plotted vs. K^2 in fig. 4. Within a fairly large experimental error, δ takes a nearly constant value of about 2.2% at $K^2 > 1.5 \times 10^{14}$ m^{-2}, where the effect of intramolecular motion is dominant. Although the measurement is made on DNA of linear form, the saturated value of δ agrees very well with the prediction from the KS theory for circular chains. Theoretically, δ should tend to zero in the small K region where $1/K$ is much larger than the chain dimension. The measured δ, however, has a small but finite positive value of about 1% even at the smallest K^2, 2.5×10^{12} m^{-2}, where the above condition holds. This result is probably caused by the incomplete elimination of the effects of light scattered by a small amount of dust particles in solution and/or stray reflection.

By making a fourth-order cumulant fitting of eq. 5 to $C(t)$, the following quantity,

$$D_s(t) = -\frac{1}{2K^2}\frac{\partial}{\partial t}(\ln f_{C4}(t)) = \frac{1}{2K^2}\left(K_1 - K_2 t + \frac{K_3}{2}t^2 - \frac{K_4}{6}t^3\right), \quad (13)$$

can be derived from the fitted function. $D_s(t)$

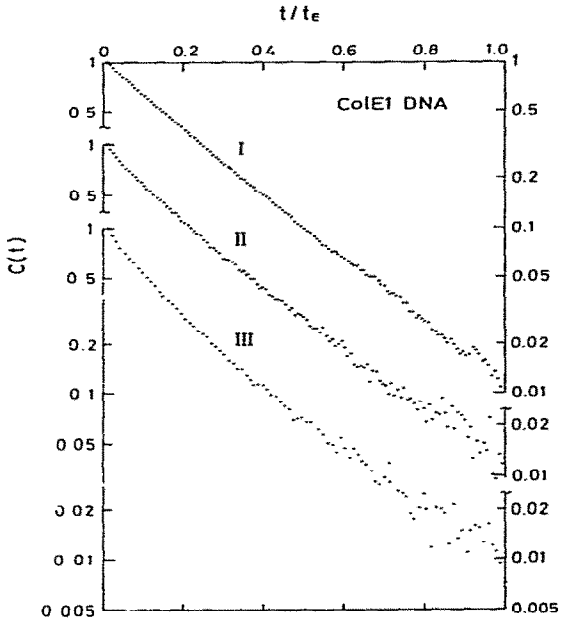

Fig. 3. Semilogarithmic plots of typical correlation functions for ColEI DNA. Scattering angles (°): (I) 11.48, (II) 36.87, (III) 90.00. Experimental conditions: 1×SSC (pH 7.0), $c = 88$ μg/ml, $T = 25.0$ °C.

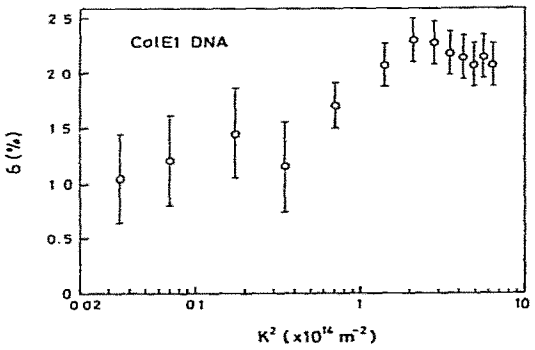

Fig. 4. δ vs. K^2 for ColEI DNA: 1×SSC (pH 7.0), $c = 75$–88 μg/ml, $T = 25.0$ °C. δ is defined by eq. 6.

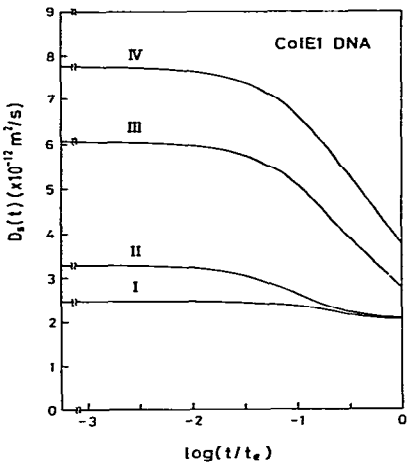

Fig. 5. $D_s(t)$ vs. normalized delay time for ColEl DNA: 1×SSC (pH 7.0), $c = 88$ μg/ml, $T = 25.0$ °C. Values of K^2 (m^{-2}): (I) 7.0×10^{12}, (II) 7.0×10^{13}, (III) 3.5×10^{14}, (IV) 6.3×10^{14}. t_ϵ is the delay time at which $C(t)$ is 1/100 of the correlation amplitude, $C(0)$.

denotes the apparent diffusion coefficient obtained from a single exponential fitting of the correlation function in the neighborhood of t. The dependence of $D_s(t)$ on t also characterizes the shape of the correlation function. $D_s(t)$ values of the above data for four values of K^2 are shown in fig. 5. $D_s(t)$ for the smallest K^2 (curve I) shows a very weak dependence on t, indicating that the correlation function is of nearly single-exponential form. On the other hand, for $K^2 = 6.3\times10^{14}$ m^{-2}, D_s at $t = 0$ amounts to about 2.1-times D_s at $t = t_\epsilon$, which is in good agreement with the estimation of 2.16 from the KS theory.

3.2. Apparent diffusion coefficients

In the following, D_a values which are given by fitting $f_{se}(t)$ in eq. 4 under the conditions that B is fixed to zero and that it is variable are denoted by D_{a0} and D_{a1}, respectively. In fig. 6 are shown the K dependences of the apparent diffusion coefficients

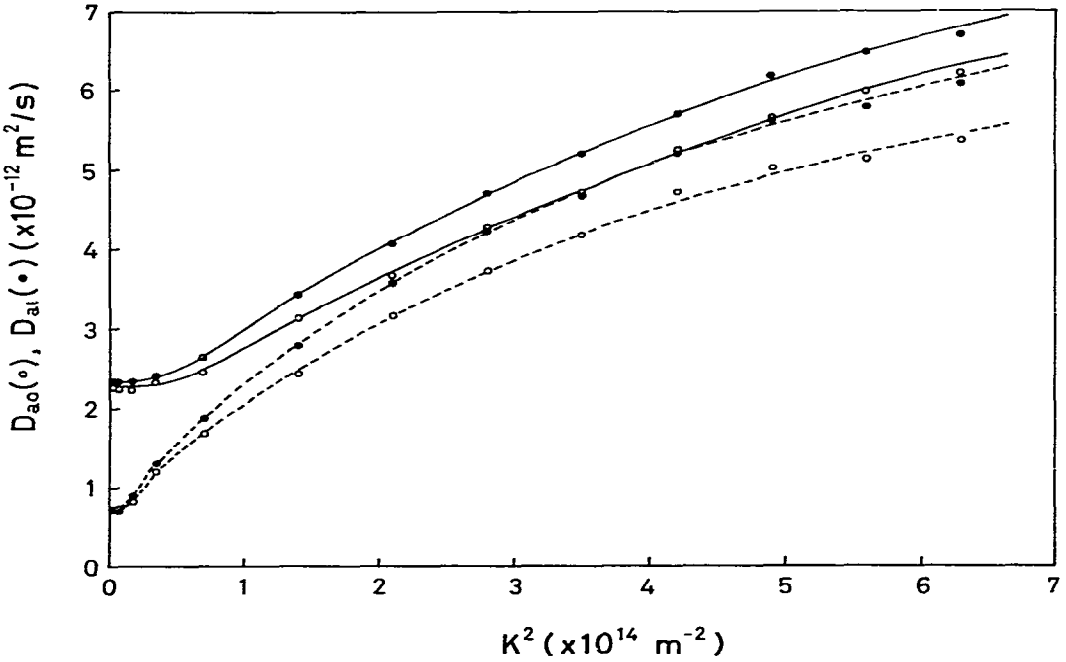

Fig. 6. Dependences of the apparent diffusion coefficients, D_{a0} and D_{a1}, on K^2: (●) D_{a1}, (○) D_{a0}. Samples: ColEl DNA (upper pair, ———), $c = 88$ μg/ml; λ-DNA (lower pair, - - - - - -), $c = 23$–27 μg/ml. Experimental conditions: 1×SSC (pH 7.0), $T = 25.0$ °C.

of both λ- and ColEl DNA. D_{a0} and D_{a1} are each an increasing function of K^2 with a curve which has an inflection point at an intermediate value of K^2 characteristic of the DNA. For example, D_{a1} at the maximum measuring angle of $\theta = 143.13°$, where $\sin^2(\theta/2) = 0.9$, amounts to about 9- and 3-times those at small angles for λ- and ColEl DNA, respectively.

If the intramolecular motion of a DNA chain is determined only by its mechanical properties, it is expected that the value of D_a at large angles, where the contribution from the internal motion is dominant, should not depend on the origin of DNA. Thomas et al. [14] reported data that D_{a1} vs. K^2 curves for ϕ29 DNA and λ-DNA ($M_r = 3.25 \times 10^7$) closely agreed with each other throughout the region $K^2 = (0.5–20) \times 10^{14}$ m^{-2} in which they made the measurement.

In our case of ColEl DNA ($M_r = 4.37 \times 10^6$) and λ-DNA, the difference between the two curves decreases with increasing K^2. However, both D_{a0} and D_{a1} of the former are significantly larger than the corresponding values of the latter even at the maximum K^2 of 6.3×10^{14} m^{-2}. This is in sharp contrast to the data of Thomas et al. Our data are considered to result from either or both of the following situations: (1) The forms of the two DNAs differ, i.e., λ-DNA is circular and ColEl DNA is linear. (2) As ColEl DNA is only about 1/8 of λ-DNA in contour length, the effect of translational motion can appear significantly in the correlation functions of ColEl DNA even at the maximum K^2.

Our data for circular λ-DNA agree well with those of Thomas et al. [14] for linear λ-DNA over the whole K^2 range except for very small K^2. This indicates that the internal motion of a DNA molecule with a sufficiently long contour length hardly depends on its chain form. The apparent diffusion coefficients do not show such a tendency to saturate in the range $K^2 < 7 \times 10^{14}$ m^{-2} as was observed earlier for insufficiently purified calf thymus DNA.

Fitting D_{a1} vs. K^2 curves obtained from the numerical calculation using the KS theory to measured data is done in fig. 7 for the circular λ-DNA. The measured D_{a1} lies between the theoretical curves for $a = 75$ and 100 nm at $K^2 < 2.1 \times 10^{14}$ m^{-2} and $K^2 > 5.6 \times 10^{14}$ m^{-2}, and takes a slightly larger value than the theoretical one for $a = 100$ nm in the intermediate K^2 region. The value of persistence length estimated from the above fitting is about 1.5–2-times the presently accepted range, 50–60 nm, obtained for DNA with a molecular weight of several million under the condition of 0.2 M NaCl. The KS theory also predicts that D_{a1} is fairly insensitive to change in the value of a. Accordingly, a small change in the theoretical curve of D_{a1} could result in a large change in the estimate of a. Several approximations noted in section 2.5 might cause such a small error in the theoretical curve of D_{a1}.

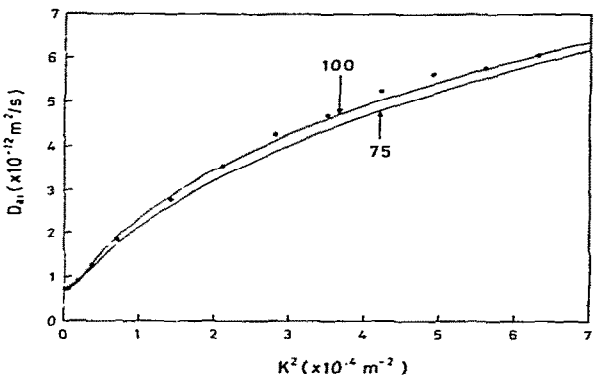

Fig. 7. Comparison between calculated D_{a1} vs. K^2 curves for a circular semiflexible chain with $L = 16.6$ μm and measured data for circular λ-DNA. The data (●) are the same as those in fig. 6. The numbers beside the curves indicate the value of the persistence length (in nm).

3.3. Exponent in the K dependence of the spectral line width

Next, we will consider the problem of the exponent in the K dependence of the spectral linewidth of scattered light. There are several quantities which are derived from the power spectrum or the correlation function, and which can be taken as a definition of the spectral linewidth. The half-width at half-maximum of the power spectrum, the characteristic frequency or the initial decay rate of the correlation function, and the decay constant of the single exponential function fitted to the correla-

tion function are the examples. In our case with DNA, the values of the spectral linewidth given by different definitions have nearly the same K dependence in the large K region where the intramolecular interference effect is significant. Therefore, there is no need to select one particular definition in the following discussion, and we will denote all the quantities characterizing the spectral linewidth as Γ_s.

Dubois-Violette and De Gennes [29] showed theoretically that, when hydrodynamic interactions between beads are taken into account, the half-width of the power spectrum for RZ chains is proportional to K^3. Akcasu and Gurol [30] showed that the characteristic frequency is also proportional to K^3. These results mean that the following relation holds for RZ chains:

$$\Gamma_s \propto K^3. \tag{14}$$

Eq. 14 was derived under the condition that the chain is so long that its translational motion can be neglected. Therefore, the condition $KR \gg 1$ was necessarily assumed, where R is the root-mean-square radius of the chain.

Lin and Schurr [11] obtained a theoretical expression of the correlation function for the RZ chain without any restriction on the applicable range of K. They found that the apparent diffusion coefficient reaches a plateau value in the K region of $Kb \gg 1$, where b is the root-mean-square distance between adjacent beads. The plateau value corresponds to the translational diffusion coefficient of a bead. The condition $KR \gg 1$ is naturally satisfied in the K region. The result obtained by Lin and Schurr means that the following relation holds in the above K region:

$$\Gamma_s \propto K^2. \tag{15}$$

They measured calf thymus DNA to provide data in support of the relation expressed by eq. 15.

In order to consider the above contradiction, a log-log plot of the data in fig. 6 is shown in fig. 8. The straight line drawn in the figure has a slope of 1/2. If the data curve is parallel to it, it means that the relation $\Gamma_s \propto K^3$ holds because, in this case, Γ_s is given by

$$\Gamma_s = D_{a1} K^2. \tag{16}$$

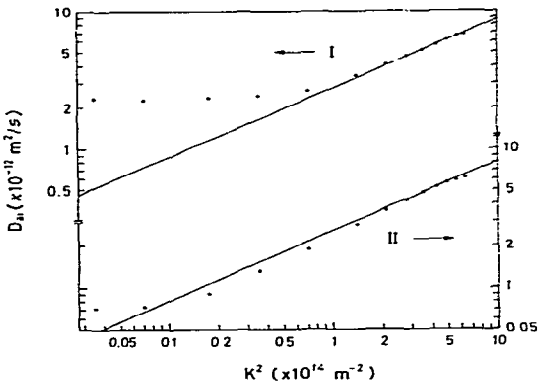

Fig. 8. Log-log plots of D_{a1} vs. K^2: (I) ColEI DNA, (II) λ-DNA. The data are the same as those in fig. 6. Each of the straight lines has a slope of 1/2 and, if the relation $\Gamma_s \propto K^3$ holds, the data should lie on a line parallel to it.

The exponent for λ-DNA is seen to be significantly larger than 3 at $K^2 = (0.3\text{–}3) \times 10^{14}$ m^{-2} and reaches a maximum of 3.2 near $K^2 \approx 1.3 \times 10^{14}$ m^{-2}. It decreases with increasing K^2, and the relation of eq. 14 holds approximately at $K^2 = (2\text{–}6) \times 10^{14}$ m^{-2}. We have no data at K^2 larger than 6.3×10^{14} m^{-2} because of the unavailability of laser light with a shorter wavelength. When the same plot is made for the data of Thomas et al. [14], it shows that the relation of eq. 14 nearly holds till $K^2 \approx 10 \times 10^{14}$ m^{-2}. This means that, in the region of $K^2 = (2\text{–}10) \times 10^{14}$ m^{-2}, the K dependence of Γ_s obeys the relation given by Dubois-Violette and De Gennes. For larger K^2, the D_a curve deviates downward from the straight line.

If we denote $(\pi/2K)$ by ρ_i, it is a quantity with the dimension of length and characterizes a measure of the spatial resolution in the light-scattering measurement at this angle. Two points at an interval shorter than ρ_i can be regarded approximately as identical points. Conversely, for scattering units separated by a distance longer than ρ_i, it must be taken into account that the mode of interference between the light scattered from them varies with their relative orientation. ρ_i is 50 nm at $K^2 = 10 \times 10^{14}$ m^{-2} near which the measured K dependence of Γ_s begins to deviate from the relation of eq. 10.

The above value of ρ_t is nearly the same as the best estimate of the persistence length of DNA under the condition of 0.2 M Na^+. From this fact, it is clear that, in a light-scattering measurement at $K^2 > 10 \times 10^{14}$ m^{-2}, the static and dynamic structures of the chain segment shorter than the Kuhn statistical segment length affect the measured results. Therefore, the experimental fact that the relation of eq. 14 is violated in the above region should be explained not by using a RZ model, but in terms of the properties of the worm-like DNA molecule.

From these results and discussion, the above contradiction regarding the exponent is interpreted as follows. Originally, the RZ model was introduced to study slow relaxational modes of a flexible polymer chain. The masses continuously distributing along the contour of a real molecule are replaced by a series of beads and massless Hookian springs in the model. Because the restoring force of the spring is an entropic one, we can safely use the model as a dynamic model only for motion that is far slower than that of segments in a real molecule. It cannot, at least in the strictest sense, be applied to phenomena in which the mass distribution inside a bead and/or the motion of segments forming the bead may be involved. Therefore, the conditions on the range of K necessary for applying the theory of Dubois-Violette and De Gennes must include not only $KR \gg 1$ but also $Kb < 1$. On the other hand, it can easily be understood that, in the large K region where the relation $Kb \gg 1$ holds, i.e., where the spatial resolution is much higher than b, each bead is seen as if it were performing thermal motion independently, which leads to the relation of eq. 15. In conclusion, the difference in exponent arises from the difference in the range of K in which $1/K$ is either larger or smaller than b.

Very recently, Schurr [31] presented quantitative criteria for determining the boundaries of the 'K^3' region and the 'K^2' region for semiflexible chains using RZ model parameters. According to his criteria, a true K^3 region can appear in the D_a vs. K^2 curve for λ-DNA. From this inference and the fact that the maximum of the exponent for λ-DNA is about 3.2, it is inferred that the exponent for a sufficiently long native DNA is larger than 3 in the K range corresponding to the K^3 region for RZ chains. This behavior of D_{a1} for λ-DNA in the K^3 region was found to agree well with the prediction from the KS theory.

Adam and Delsanti [32] obtained an exponent of 2.85 for a flexible coil molecule of polystyrene in an organic solvent. The fact that the exponent for λ-DNA is larger than 3 at $K^2 < 3 \times 10^{14}$ m^{-2} is in marked contrast to the result on polystyrene. Probably, this is a manifestation of the worm-like nature of native DNA molecules.

Details of the K dependence of the apparent diffusion coefficient in the K range much higher than the K^3 region have yet to be elucidated both experimentally and theoretically. Schurr [31] assumed that the apparent diffusion coefficient of a semiflexible chain reaches a plateau value at sufficiently large K and called this K region the plateau region. Thomas et al. [14] estimated the plateau value of the apparent diffusion coefficient for ϕ29 DNA from DLS data up to $K^2 \approx 20 \times 10^{14}$ m^{-2} and, using this value, they obtained the values of RZ model parameters. However, even if the apparent diffusion coefficient really reaches a plateau value at very large K^2, it seems difficult to us to estimate accurately the true plateau value from their data. Recently, Wilcoxon and Schurr [33] found that D_i of a thin rod does reach a plateau value at very large K^2, but the approach to it with increasing K is extremely slow.

3.4. *Effect of concentration and translational diffusion coefficient*

Let us consider next the effect of solute concentration on the K^2 dependence of D_a. For this purpose, we define the volume, v_s, of a sphere equivalent to a DNA molecule by

$$v_s = (4\pi/3) R^3. \tag{17}$$

The mean volume per solute molecule, v_m, is given by

$$v_m = M/N_A c, \tag{18}$$

where c, M and N_A are the concentration, molecular weight, and Avogadro's number, respectively.

D_{a1} vs. K^2 curves for ColEl DNA at two con-

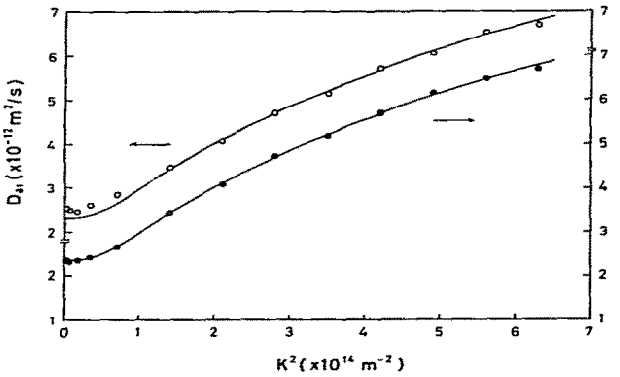

Fig. 9. Dependence of D_{a1} on K^2 at two different concentrations of ColEI DNA: (●) 75 μg/ml, (○) 155 μg/ml. Experimental conditions: 1×SSC (pH 7.0), $T = 25.0$ °C. Each solid line is the curve passing through the data on the sample with $c = 75$ μg/ml.

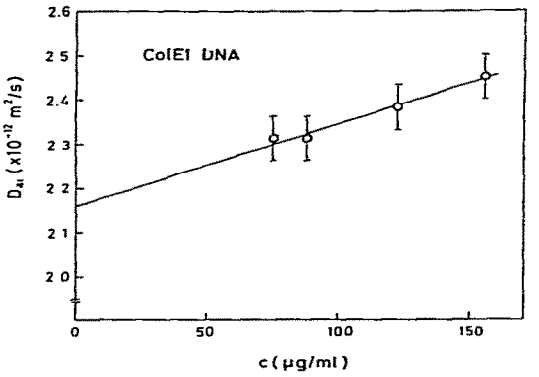

Fig. 10. Dependence of D_{a1} extrapolated to $K = 0$ on concentration for ColEI DNA: 1×SSC (pH 7.0), $T = 25.0$ °C.

centrations are shown in fig. 9. Voordouw et al. [12] obtained the value of R as 186 nm for linear ColEI DNA in 0.2 M NaCl from a static light-scattering measurement. Adopting their value of R, we have $v_s = 2.70 \times 10^{-2}$ μm^3. v_m values are given as 9.65 and 4.69×10^{-2} μm^3 and the percentages of v_s to v_m are 28 and 58% for the respective concentrations. The two curves in the figure agree well with each other in the region of $K^2 > 1.4 \times 10^{14}$ m^{-2}, and the effect of the intermolecular interaction on the intramolecular motion is seen to be very small even in this range of concentration. On the other hand, at smaller K^2, D_{a1} is significantly larger in the case of higher concentration. Further, it was observed that the deviation of the correlation function from a single exponential function was also larger for higher concentration. The above result indicates that the effect of cooperative diffusion begins to be manifested.

The value of D_{a1} extrapolated to $K = 0$ is plotted vs. concentration in fig. 10. By assuming a linear dependence of D_{a1} on concentration, the extrapolation to $c = 0$ yields an estimate of $D^0_{25,w} = (2.16 \pm 0.1) \times 10^{-12}$ m^2/s for the translational diffusion coefficient at infinite dilution. This is about 4% lower than the value of $D^0_{25,w} = 2.26 \times 10^{-12}$ m^2/s which is obtained by reducing the value measured at 20 °C by Voordouw et al. However, their D_a takes values slightly larger than our D_{a1} throughout the region of K^2. As the details of the process for obtaining D_a in their data analysis have not been described, it is meaningless to compare our values and theirs closely.

In fig. 11 are shown D_{a1} vs. K^2 curves of

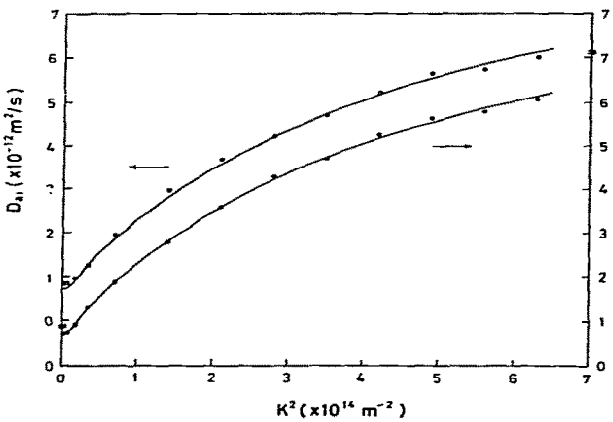

Fig. 11. Dependence of D_{a1} on K^2 at two different concentrations of λ-DNA: (lower curve) 27 μg/ml, (upper curve) 92 μg/ml. Experimental conditions: 1×SSC (pH 7.0), $T = 25.0$ °C. Each solid line is the curve passing through the data on the sample with $c = 27$ μg/ml.

λ-DNA. The values of v_m at two concentrations in this figure are 2.02 and 0.59 μm^3. Dawson and Harpst [22] obtained a value of R for open circular λ-DNA as 680 nm, which leads to $v_s = 1.32$ μm^3. This implies that the solute molecules in our sample with higher concentration overlap each other. However, substitution of the values of R and L into the expression for a sufficiently long circular chain, $R \approx (aL/6)^{1/2}$, gives a value of the apparent persistence length of 167 nm. This seems too large even if the excluded volume effect is taken into account. If, for example, a value of 60 nm is taken for a. R and v_s become 408 nm and 0.29 μm^3, respectively, and the overlapping nearly disappears.

Both curves in the figure agree within experimental error at K^2 larger than the limit of about 3×10^{13} m^{-2}, which is much smaller than that for ColEl DNA. This result also indicates that the internal motion is made almost independent of the intermolecular interaction. The behavior of the curves at smaller K^2 is qualitatively the same as that for ColEl DNA. Although the degree of dilution might not be sufficient, we obtain an estimate of the value of the translational diffusion coefficient of $D_{25,w} = 7.1 \times 10^{-13}$ m^2/s by extrapolating the curve of lower concentration to $K^2 = 0$. The substitution of $s^0_{20,w} = 39.2$ S, $\partial\rho/\partial c = 0.457$, and $M_r = 3.25 \times 10^7$ into the Svedberg equation,

$$D = \frac{sRT}{M_r(\partial\rho/\partial c)}, \tag{19}$$

leads to $D^0_{20,w} = 6.43 \times 10^{-13}$ m^2/s, which is reduced to give $D^0_{25,w} = 7.37 \times 10^{-13}$ m^2/s. The value of the translational diffusion coefficient obtained from DLS is about 4% lower than that from the velocity sedimentation.

3.5. *Effects of ionic strength and temperature*

In recent years, data indicating that the persistence length of DNA has a fairly strong dependence on ionic strength have been obtained from measurements of flow birefringence [34] and static light scattering [35]. Schmitz [36] and Parthasarathy and Schmitz [37] reported that, for calf thymus DNA, its DLS properties showed significant dependences on both ionic strength and salt type.

In order to elucidate the effect of ionic strength on DLS, measurements were made on samples with three different salt concentrations (fig. 12). No difference between the curves for 10 × SSC buffer (1.95 M Na^+) and 3 × SSC buffer (0.585 M Na^+) was found within experimental error. The D_{a1} value for 1 × SSC buffer takes only slightly higher values than those for 10 × and 3 × SSC buffer at large K^2. According to the data of Borochov et al. [35], the ratio of the apparent persistence length in 0.2 M Na^+ to that in 2 M Na^+ is 49.8 nm/34.1 nm = 1.46. Our data show that the effect of ionic strength in the above range on DLS properties is negligible. In spite of some quantitative differences, the result of the ionic strength dependence of our ColEl DNA sample is qualitatively similar to those of erythrocyte DNA obtained by Caloin et al. [38] and of φ29 DNA by Thomas et al. [14,39].

The persistence length, a, is determined by the bending rigidity of DNA, ϵ, and temperature and is given by

$$a = \epsilon/kT. \tag{20}$$

Therefore, the amplitude of the structural fluctua-

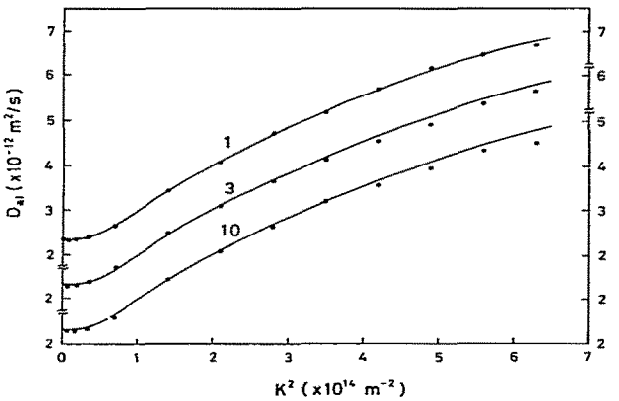

Fig. 12. Dependence of D_{a1} on K^2 for ColEl DNA in three SSC buffers with different salt concentrations ($T = 25.0$ °C). The number above each curve indicates the salt concentration in SSC units. Each solid line is the curve passing smoothly through the data on the sample in 1 × SSC buffer. DNA concentrations of the samples in 1, 3 and 10 × SSC buffers: 88, 67 and 78 μg/ml, respectively.

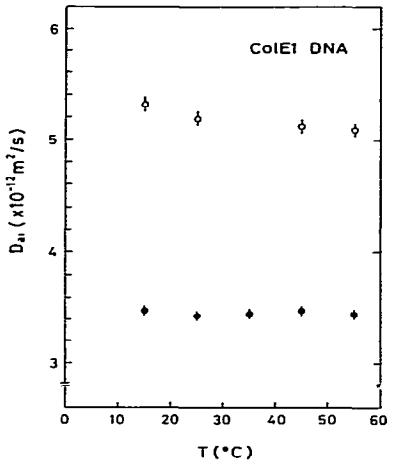

Fig. 13. Temperature dependence of D_{a1} at two scattering angles for ColEl DNA in 1×SSC buffer: (●) $\theta = 53.16°$ ($K^2 = 1.4 \times 10^{14}$ m^{-2}), (○) $\theta = 90.00°$ ($K^2 = 3.5 \times 10^{14}$ m^{-2}). DNA concentration, 87 μg/ml.

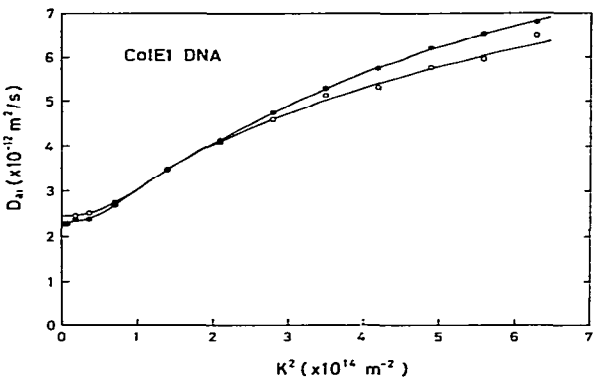

Fig. 14. Dependence of D_{a1} on K^2 for ColEl DNA at two different temperatures. (●) $T = 15.0°$C, (○) $T = 55.0°$C. Experimental conditions: 1×SSC buffer, $c = 81$–87 μg/ml.

tion and the magnitude of the intramolecular hydrodynamic interaction are expected to be altered on change in solution temperature. In order to demonstrate this effect, the temperature dependence of D_{a1} at two values of K^2 is shown in fig. 13. D_{a1} takes a value remaining constant to 0.7% at temperatures between 15 and 55°C at $K^2 = 1.4 \times 10^{14}$ m^{-2} where $\sin^2(\theta/2) = 0.2$. On the other hand, at $K^2 = 3.5 \times 10^{14}$ m^{-2} where $\sin^2(\theta/2) = 0.5$, D_{a1} at 55°C is 4.3% lower than that at 15°C, which is a significant difference exceeding experimental error. This result implies that the effect of temperature on D_{a1} can differ with the scattering angle or the value of K^2.

To elucidate the K dependence of the temperature effect, D_{a1} values measured at 15 and 55°C are plotted in fig. 14. D_{a1} for 15°C is larger than that for 55°C at $K^2 > 2.1 \times 10^{14}$ m^{-2} and vice versa at $K^2 < 0.7 \times 10^{14}$ m^{-2}. Both curves nearly agree in the intermediate region between the above boundaries. In the large K^2 region, the difference between them becomes larger with increasing K^2. At our maximum K^2 of 6.3×10^{14} m^{-2}, it amounts to 5.5×10^{-13} m^2/s which is more than 8% of the mean value of D_{a1}. If we assume that the bending rigidity of a chain does not change with temperature, theoretical values of D_{a1} at different temperatures can be estimated from the KS theory. According to the result of the numerical calculation for a model chain corresponding to circular ColEl DNA, the relation between the magnitudes of D_{a1} values at 15 and 55°C exhibits a K dependence similar to that for the measured D_{a1} values. However, the difference between the measured D_{a1} values was found to be more than twice the difference between the theoretical D_{a1} values in the large K region. Strictly speaking, the KS theory cannot be applied to a linear chain. However, the internal motion of a sufficiently long chain is expected to vary only slightly with chain form. Therefore, it is also expected that the effect of chain form on the difference between D_{a1} values at the two temperatures is small in the large K region where the internal motion dominates $S(K,t)$. If this inference is correct for ColEl DNA, then the experimental result means that the stiffness of native DNA varies with temperature in the temperature range substantially lower than that of melting.

Recently, Wilcoxon and Schurr [40] reported that the apparent diffusion coefficient of φ29 DNA hardly depends on temperature in the temperature range from −0.5 to 70°C. They found that significant degradation of DNA had occurred during the long course of a measurement at a temperature

higher than about 40 °C. They noted that it is essential to find appropriate buffer conditions for avoiding degradation of DNA. If such degradation could also occur in SSC buffers, it would exert a substantial effect on the DLS properties of our DNA samples.

Hoff and Blok [41] reported that heating at 70 °C produced single strand breaks at a rate of about 1.7 breaks/molecule per h for T4 DNA ($M_r = 1.3 \times 10^8$) in 10 mM phosphate buffer containing 1 mM EDTA. If single strand breaks occurred in SSC buffers at the same rate as the above, a 24-h heating of ColEl DNA at 70 °C would yield only about 1.4 single strand breaks per molecule. Therefore, if this is the case in our experiments, the effect of DNA degradation is expected to be negligible, because the buffer conditions of Hoff and Blok are much more severe than ours (1 × SSC, 55 °C) in both ionic strength and temperature.

The effect of DNA degradation was determined to be negligible in our case from the following results: (1) The correlation functions measured at $\theta = 25.8$ and 90.0° immediately after heating to 55 °C agreed quite well with those measured after a 24-h run at 55 °C; and (2) no detectable difference was found between the ColEl DNA kept at 55 °C for 20 h and that without heating in the patterns of both non-denaturing and denaturing agarose gel electrophoresis. Thus, the origin of the discrepancy between the data of Wilcoxon and Schurr, and ours remains unknown at present.

References

1 V.A. Bloomfield, D.M. Crothers and I. Tinoco, Jr, Physical chemistry of nucleic acids (Harper & Row, New York, 1974) p. 151.
2 R.I. Schmidt, Biopolymers 12 (1973) 1427.
3 K.S. Schmitz and J.M. Schurr, Biopolymers 12 (1973) 1543.
4 K.S. Schmitz and R. Pecora, Biopolymers 14 (1975) 521.
5 K.L. Wun and W. Prins, Biopolymers 14 (1975) 111.
6 R.L. Schmidt, J.A. Boyle and J.A. Mayo, Biopolymers 16 (1977) 317.
7 W.I. Lee, K.S. Schmitz, S.-C. Lin and J.M. Schurr, Biopolymers 16 (1977) 583.
8 D. Jolly and H. Eisenberg, Biopolymers 15 (1976) 61.
9 F.C. Chen, A. Yeh and B. Chu, J. Chem. Phys. 66 (1977) 1290.
10 R. Pecora, J. Chem. Phys. 49 (1968) 1032.
11 S.-C. Lin and J.M. Schurr, Biopolymers 17 (1978) 425.
12 G. Voordouw, Z. Kam, N. Borochov and H. Eisenberg, Biophys. Chem. 8 (1978) 171.
13 J.C. Thomas and J.M. Schurr, Opt. Lett. 4 (1979) 222.
14 J.C. Thomas, S.A. Allison, J.M. Schurr and R.D. Holder, Biopolymers 19 (1980) 1451.
15 S.C. Lin, J.C. Thomas, S.A. Allison and J.M. Schurr, Biopolymers 20 (1981) 209.
16 O.G. Berg, Biopolymers 18 (1979) 2861.
17 A.R. Goldberg and M. Howe, Virology 38 (1969) 200.
18 Y. Sakakibara and J. Tomizawa, Proc. Natl. Acad. Sci. U.S.A. 71 (1974) 802.
19 O.H. Lowry, N.J. Rosebrough, A.L. Farr and R.J. Randall, J. Biol. Chem. 193 (1951) 265.
20 O. Gotoh, Y. Husimi, S. Yabuki and A. Wada, Biopolymers 15 (1976) 655.
21 J.C. Wang and N. Davidson, J. Mol. Biol. 15 (1966) 111.
22 J.R. Dawson and J.A. Harpst, Biopolymers 10 (1971) 2499.
23 A.I. Krasna and J.A. Harpst, Proc. Natl. Acad. Sci. U.S.A. 51 (1964) 36.
24 L.W. Tilton and J.K. Taylor, J. Res. Nat. Bur. Stan. 20 (1938) 419.
25 T. Maeda and S. Fujime, Macromolecules 14 (1981) 809.
26 R. Fletcher and M.J.D. Powell, Computer J. 6 (1963) 163.
27 D.E. Koppel, J. Chem. Phys. 57 (1972) 4814.
28 H. Yamakawa and M. Fujii, Macromolecules 6 (1973) 407.
29 E. Dubois-Violette and P.G. De Gennes, Physics 3 (1967) 181.
30 Z. Akcasu and H. Gurol, J. Polym. Sci. Polym. Phys. 14 (1976) 1.
31 J.M. Schurr, Biopolymers 22 (1983) 2207.
32 M. Adam and M. Delsanti, Macromolecules 10 (1977) 1229.
33 J. Wilcoxon and J.M. Schurr, Biopolymers 22 (1983) 849.
34 R.E. Harrington, Biopolymers 17 (1978) 919.
35 N. Borochov, H. Kam and H. Eisenberg, Biopolymers 20 (1981) 231.
36 K.S. Schmitz, Biopolymers 18 (1979) 479.
37 N. Parthasarathy and K.S. Schmitz, Biopolymers 19 (1980) 1655.
38 M. Caloin, B. Wilhelm and M. Daune, Biopolymers 16 (1977) 2091.
39 J.C. Thomas and J.M. Schurr, Biopolymers 19 (1980) 215.
40 J. Wilcoxon and J.M. Schurr, Biopolymers 22 (1983) 2273.
41 A.J. Hoff and J. Blok, Biopolymers 9 (1970) 1349.
42 K. Soda, Macromolecules (1984) in the press.